

Effect of Block Sequence on the Self-Assembly of ABC Terpolymers in Selective Solvent

Yi Zhang, Wencheng Lin, Rongkuan Jing, and Junlian Huang*

*The Key Laboratory of Molecular Engineering of Polymer, State Education Ministry of China, Department of Macromolecular Science, Fudan University, Shanghai 200433, China**Received: June 17, 2008; Revised Manuscript Received: October 12, 2008*

The effect of block sequence on the self-assembly of ABC terpolymers in selective solvent (water/THF) was explored based on two kinds of terpolymers: polystyrene-*block*-poly(ethylene oxide)-*block*-poly(acrylic acid) (PS-*b*-PEO-*b*-PAA) and PEO-*b*-PS-*b*-PAA with the same component, comparable molecular weight, but different block sequence. Copolymer PS-*b*-PEO-*b*-PAA has a higher critical water content (CWC) and larger aggregates size than PEO-*b*-PS-*b*-PAA. Furthermore, they presented vesicles with hundreds of nanometers at 25% water content which was not observed in the case of PEO-*b*-PS-*b*-PAA. It was also found that there was a sharp jump of both the scattering light intensity and average aggregate size for PS-*b*-PEO-*b*-PAA. The kinetics of morphological transitions vs the water content was described to explain this phenomenon.

Introduction

In the past several decades, the research on the self-assembly of block copolymers in selective solvent for one of the blocks forming core or aggregating as a result of association of the insoluble blocks is gaining increasing attention.^{1–4} Such self-assembly processes are driven by diverse repulsion forces including the stretching (deformation) of the core-forming blocks in the core, the surface tension between the micelle core and the solvent outside of the core, and the intercorona–chain interactions.⁵ Star micelles^{6,7} and crew-cut aggregates^{8,9} should be distinguished: the former is usually made from block copolymers in which the corona-forming blocks are much longer than the core-forming blocks, while the latter is made from copolymers in which the core-forming blocks are much longer. It has been known that the star micelles are usually spherical,¹⁰ while the crew-cut aggregates have self-assembled into structures with various morphologies.^{11,12}

By now the self-assembly of AB diblock copolymers has been studied widely and systematically.^{13–15} The copolymers used for this research include poly(styrene)-*b*-poly(acrylic acid),^{16,17} poly(styrene)-*b*-poly(ethylene oxide),^{18,19} and other copolymer systems.^{20–22} ABC terpolymers are also versatile precursors of micelles,^{23–26} whose structure is dictated by the constitutive blocks and their sequential arrangement. Because of consisting of three chemically different blocks which can be multiresponsive or sufficiently incompatible with each other, smart materials made by ABC terpolymers can be contemplated. Recently, there has been considerable interest in exploring the solution behavior of ABC terpolymers,^{27,28} and a variety of nano-objects in dilute solutions have been obtained, ranging from typical core–shell nanospheres²⁹ to cylinders and vesicles.³⁰ Traditionally, the studies on self-assembly of ABC terpolymers in selective solvent mainly focused on changing the environmental conditions, such as salt concentration,²⁴ pH,^{23,31} ratio of selective solvent in total solution,³² temperature,²⁵ and so on. It is worthy to be expected that the variation of arrangement sequence of ABC terpolymers may exert great influence on the aggregate behavior of these copolymers, but there are few examples among current research.

One of the reasons limiting the exploration is that it is hard to obtain copolymers with the same component, comparable molecular weight, but different block sequence ($A_nB_mC_p$, $A_nC_pB_m$, $B_mA_nC_p$). Furthermore, the existing reports^{33–36} were confined to the effect of block sequence on the hydrodynamic diameters and cloud points of the samples including critical water content (CWC) and critical solution temperature (an upper or lower critical solution temperature), but none of these examples provided convincing proof of the morphological variety induced by variation of arrangement sequence of copolymers.

In this paper, two ABC terpolymers, PS-*b*-PEO-*b*-PAA and PEO-*b*-PS-*b*-PAA, were used to investigate the effect of block sequence on the self-assembly of ABC terpolymers in H₂O/THF, including CWC, hydrodynamic diameters, and morphology, especially.

Experimental Section

Materials. The syntheses of ABC terpolymers [polystyrene-*block*-poly(ethylene oxide)-*block*-poly(*tert*-butyl acrylate)³⁷ (PS-*b*-PEO-*b*-P tBA) and poly(ethylene oxide)-*block*-polystyrene-*block*-poly(*tert*-butyl acrylate)³⁸ (PEO-*b*-PS-*b*-P tBA)] with the same components, comparable molecular weight, and different block sequence are described elsewhere (see Supporting Information for details). The molecular weights of each copolymer are PS₁₁₅-*b*-PEO₇₀-*b*-PtBA₄₁ and PEO₇₀-*b*-PS₁₀₂-*b*-PtBA₄₁, respectively (the suffixes are the numbers of repeated unit). Trifluoroacetic acid (TFA, AR, 99%), methylene dichloride (CH₂Cl₂, AR, 99%), tetrahydrofuran (THF, AR, 99%), and sodium hydroxide (NaOH, AR) were used as received.

Measurements. ¹H NMR spectra were obtained by a DMX 500 MHz spectrometer using tetramethylsilane (TMS) as the internal standard and DMSO-*d*₆ as the solvent. Transmission electron microscope (TEM) morphology study was performed on a Hitachi H-600 electron microscope operated at an accelerating voltage of 75 kV. Dynamic light scattering (DLS) measurement was performed at 25 °C on a Malvern Autosizer 4700 dynamic light scattering instrument.

Preparation of Terpolymers PS-*b*-PEO-*b*-PAA. 4.4 g of PS-*b*-PEO-*b*-PtBA (0.2 mmol) and 3 mL (41 mmol) of trifluoroacetic acid (TFA) were dissolved in 50 mL of CH₂Cl₂

* To whom correspondence should be addressed. E-mail: jlhuang@fudan.edu.cn.

and stirred at room temperature for 36 h. After all volatiles were removed under reduced pressure, the pale gray residue PS-*b*-PEO-*b*-PAA was dried at 50 °C under vacuum for 24 h. ¹H NMR (DMSO-*d*₆, δ, ppm): 0.80–2.20 (m, –CH₃, –CH₂– of TEMPO group, –CH₂CH– of *t*BA, and –CH₂CH– of PS main chain), 2.22 (s, 1H, –CH₂CH– of *t*BA), 3.53–3.80 (m, CH₂CH₂O– of PEO chain), 4.33 (m, –C(CH₃)₂–COO–CH₂–), 6.30–7.20 (m, the phenyl of PS main chain), 7.40, 7.50, 7.90 (the residual phenyl group of the initiator BPO).

Preparation of Terpolymers PEO-*b*-PS-*b*-PAA. 1 g of PEO-*b*-PS-*b*-P *t*BA (0.05 mmol) and 1 mL (13 mmol) of trifluoroacetic acid (TFA) were dissolved in 15 mL of CH₂Cl₂ and stirred at room temperature for 36 h. All volatiles were removed under reduced pressure, and the pale gray residue PEO-*b*-PS-*b*-PAA was dried at 50 °C under vacuum for 24 h. ¹H NMR (DMSO-*d*₆, δ, ppm): 0.80–2.20 (m, –CH₃, –CH₂– of TEMPO group, –CH₂CH– of *t*BA, –CH₂CH– of PS main chain, and –C(CH₃)₂–COO–CH₂–CH₃), 2.22 (s, 1H, –CH₂CH– of *t*BA), 3.53–3.80 (m, –CH₂CH₂O– of PEO chain), 4.02 (s, –C(CH₃)₂–COO–CH₂–CH₃), 4.28 (s, –CH₂CH–N–), 6.30–7.20 (m, the phenyl of PS main chain).

Preparation of Sample Solution. The proper amount of copolymers was dissolved in THF, followed by adding acidified water with pH 3.2, 5.4, and 8.3 dropwise (1 drop/13 s) to copolymer solutions under vigorous stirring. After the addition of all the water to the organic phase, each resulting solution was vigorously stirred for an additional 24 h. The copolymers concentration was kept constant at 1 mg/mL, while the water content was varied from 5% to 50% v/v of the total solution. The experiment was carried out at 32 °C.

Characterization of Sample Solutions. 1 mg/mL of copolymer solutions in H₂O/THF were characterized in terms of their hydrodynamic diameters using dynamic light scattering. For TEM characterizations, a drop of sample solutions was deposited on carbon films supported by copper grids which were placed at 50 °C under vacuum to remove excess solvent quickly.

Results and Discussion

Polymer Synthesis and Confirmation of Structure. In order to minimize the amount of impurities in ABC triblock terpolymers (PS-*b*-PEO-*b*-PAA and PEO-*b*-PS-*b*-PAA), great attention was paid to the purification of the final copolymers (PS-*b*-PEO-*b*-P *t*BA and PEO-*b*-PS-*b*-P *t*BA) during the whole synthesis process; no diblock copolymers could be detected.^{37,38} The molecular weight of PS-*b*-PEO-*b*-PAA and PEO-*b*-PS-*b*-PAA was measured by gel permeation chromatography (GPC) and NMR, respectively, and the copolymer composition was calculated by ¹H NMR spectroscopy. Figure 1 shows the ¹H NMR spectra and the theoretical chemical structure of the copolymers PEO-*b*-PS-*b*-PAA(A) and PS-*b*-PEO-*b*-PAA(B) along with the relevant peak assignment. To obtain the reliable molecular weight of terpolymers, the *M*_n of terpolymers was calculated by the following equation from ¹H NMR:

$$M_{n(\text{PS-}b\text{-PEO-}b\text{-PAA})} = \frac{4A_g M_{n(\text{PEO})}}{A_c} \times 72 + M_{n(\text{PS-}b\text{-PEO})} \quad (1)$$

where *A*_g and *A*_c represent the integral area of the methenyl proton on the PAA main chains and all protons of the PEO main chain, respectively. *M*_{n(PEO)} and *M*_{n(PS-*b*-PEO)} are the *M*_n of PEO homopolymer and the *M*_n of PS-*b*-PEO diblock copolymer, which are obtained from refs 37 and 38 (see the Supporting Information). 44 and 72 are the molecular weight (*M*_w) of

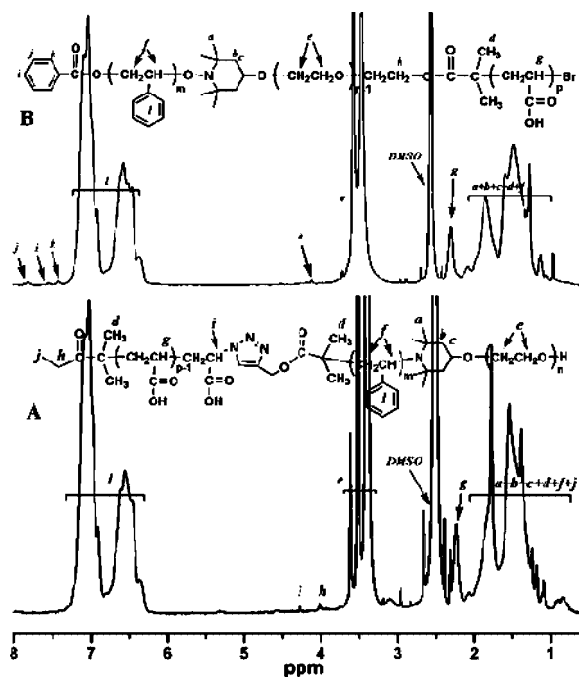


Figure 1. ¹H NMR spectra of PEO-*b*-PS-*b*-PAA(A) and PS-*b*-PEO-*b*-PAA(B) in DMSO.

TABLE 1: Polymerization Data of PS-*b*-PEO-*b*-PAA and PEO-*b*-PS-*b*-PAA

copolymer	<i>M</i> _{n,GPC} ^a (×10 ³)	<i>M</i> _n ^b (×10 ³)	<i>M</i> _w / <i>M</i> _n ^a	DP		
				PS	PEO	PAA
PS- <i>b</i> -PEO- <i>b</i> -PAA	17.7	18.1	1.32	115	70	41
PEO- <i>b</i> -PS- <i>b</i> -PAA	15.8	16.7	1.17	102	70	41

^a Determined by GPC calibrated against PS standards. ^b Determined by ¹H NMR.

ethylene oxide and acrylate acid, respectively. All the data are listed in Table 1.

Critical Water Content (CWC). The CWC is defined as the minimum amount of water needed for the micelles to start to be formed. A sudden change was observed in the intensity of scattering light as the water was added slowly.³⁹ Figure 2 shows the scattering light intensity as a function of water content at 1 mg/mL polymer concentration. As shown in Figure 2, regardless of the pH value of water, the CWC for PS-*b*-PEO-*b*-PAA was 20% (v/v), whereas 25% (v/v) for PEO-*b*-PS-*b*-PAA. There seems to be a relationship between CWC and the block sequence of ABC terpolymers. Water is a selective solvent for PEO and PAA segments; therefore, PEO and PAA blocks are stretched in the mixtures of H₂O and THF, but the hydrophobic block PS is inclined to aggregate. For PEO-*b*-PS-*b*-PAA with PS as the middle block, PEO and PAA blocks dissolved in water can more efficiently shield the PS segment from precipitant than the case of PS-*b*-PEO-*b*-PAA with PS as the end block as shown in Scheme 2. For the latter case, PS segment at one side of the polymer chain is easier to contact with the water, which is adverse for minimization of the energy; therefore, PS-*b*-PEO-*b*-PAA is more inclined to aggregate at the same water content. So a higher CWC for PEO-*b*-PS-*b*-PAA was obtained.

In addition, it should be noted that, for PS-*b*-PEO-*b*-PAA, when the CWC reached to 20%, a sharp jump in the scattering light intensity was observed regardless of pH value of water. This phenomenon will be analyzed with a combination of the following data.

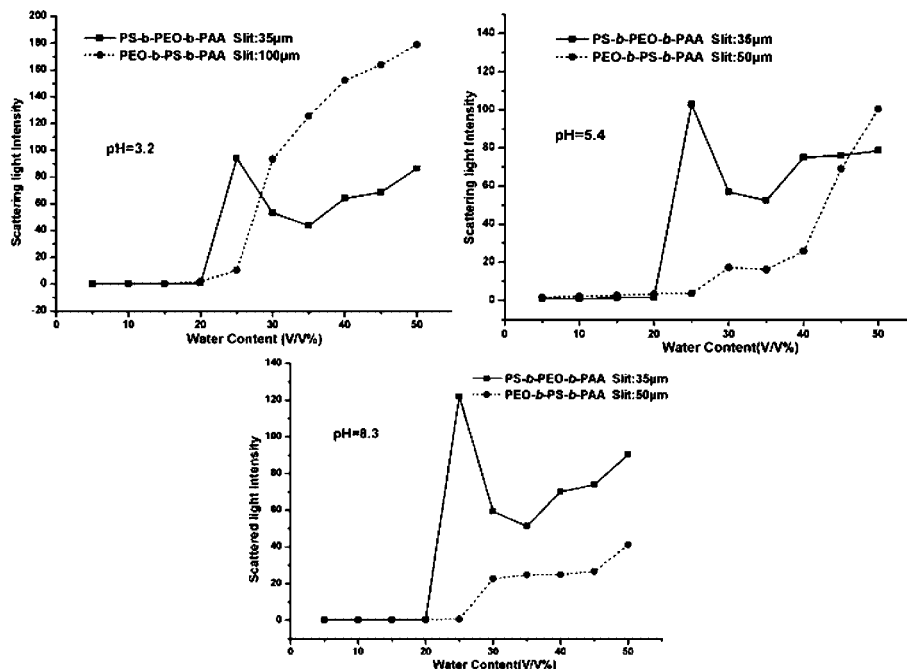
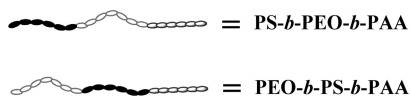
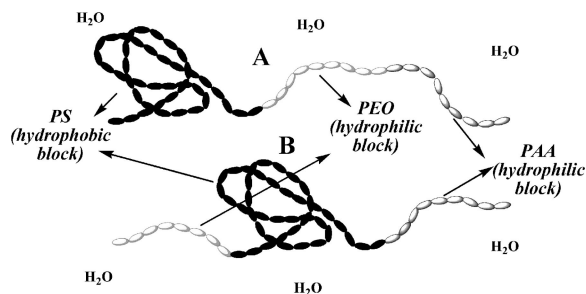


Figure 2. Scattering light intensity as a function of added water content at 1 mg/mL polymer concentration.

SCHEME 1: Schematic Drawing of the Structures of Copolymers PS-*b*-PEO-*b*-PAA and PEO-*b*-PS-*b*-PAA



SCHEME 2: Copolymers PS-*b*-PEO-*b*-PAA (A) and PEO-*b*-PS-*b*-PAA (B) in Solvent (H₂O/THF)



Hydrodynamic Diameters of Aggregates. Figure 3 contains plots of aggregates size as a function of added water content at 1 mg/mL polymer concentration for different pH. It was observed that the aggregates formed by terpolymer PS-*b*-PEO-*b*-PAA exhibited a larger size than PEO-*b*-PS-*b*-PAA in all experimental condition. This may also attribute to the different block sequence. For PS-*b*-PEO-*b*-PAA, the hydrophobic PS block was at the end of polymer chain, and the hydrophilic PEO and PAA blocks were on the another side of the chain; thus, the formed micelles were very similar to that of AB diblock amphiphilic copolymer as shown in Scheme 3A. However, for PEO-*b*-PS-*b*-PAA with the hydrophobic PS block as the middle block, it should form similar micelles formed by ABA triblock copolymers (Scheme 3B). The former micelles formed by “stretching” polymer chain have larger size than the latter ones formed through a “curving” mode in the comparable molecular weight. Similar results were also reported by others.^{32,33}

It must be emphasized that, for PS-*b*-PEO-*b*-PAA, the average size of aggregates at 25% (v/v) water content, which was just above its CWC, was extremely larger than that at other water

contents. This phenomenon corresponds to the sharp jump of scattering light intensity at the same condition. To explain the mutation, a further investigation about morphology with TEM was explored as follows.

Aggregate Morphology of the Copolymers in Mixtures of H₂O and THF. Figures 4 and 5 show the TEM pictures of the aggregates of the terpolymers PS-*b*-PEO-*b*-PAA and PEO-*b*-PS-*b*-PAA at different water content, respectively (pH value of the added water was 3.2). For PS-*b*-PEO-*b*-PAA, as shown in Figure 4A–C, the coexistence of micelles with tens of nanometers and vesicles with hundreds of nanometers was observed at 25% (v/v) water content, which illuminated the mutation in average aggregate size and scattering light intensity at the same point. When water content increased to 30% (Figure 4D,E), the number and size of the vesicles were decreased greatly compared with spherical micelles on the background. When the water content reached to 50%, only spherical micelles with tens of nanometers were obtained (Figure 4F). However, only spherical micelles formed by terpolymer PEO-*b*-PS-*b*-PAA were observed at all water contents according to Figure 5.

Figure 6 contains hydrodynamic diameter distributions $f(D_h)$ of the aggregates for PS-*b*-PEO-*b*-PAA(A) and PEO-*b*-PS-*b*-PAA(B) at different water contents (pH value of the added water was 3.2). Figure 6A shows PS-*b*-PEO-*b*-PAA chains forming aggregates with bimodal distribution at 25% water content, corresponding to the coexistence of micelles and vesicles (Figure 4A–C). Although a bimodal distribution could also be observed at 30%, the integral area of peak with larger size was decreased greatly compared with the peak at smaller size, which is coincident with the great decrease of number and size of the vesicles in TEM images (Figure 4D,E). At 50% water content, a unimodal distribution of aggregates appeared, corresponding to only micelles existence in the Figure 4F. For PEO-*b*-PS-*b*-PAA, as Figure 6B shows, the aggregates were constituted by a unimodal distribution with a peak at $D_h = 60$ nm, which is in accordance with micelles only in Figure 5.

Traditionally, a lot of researches reported the variation of the common morphology of the aggregates from spheres to rodlike micelles, to interconnected rods, and then to bilayers formed

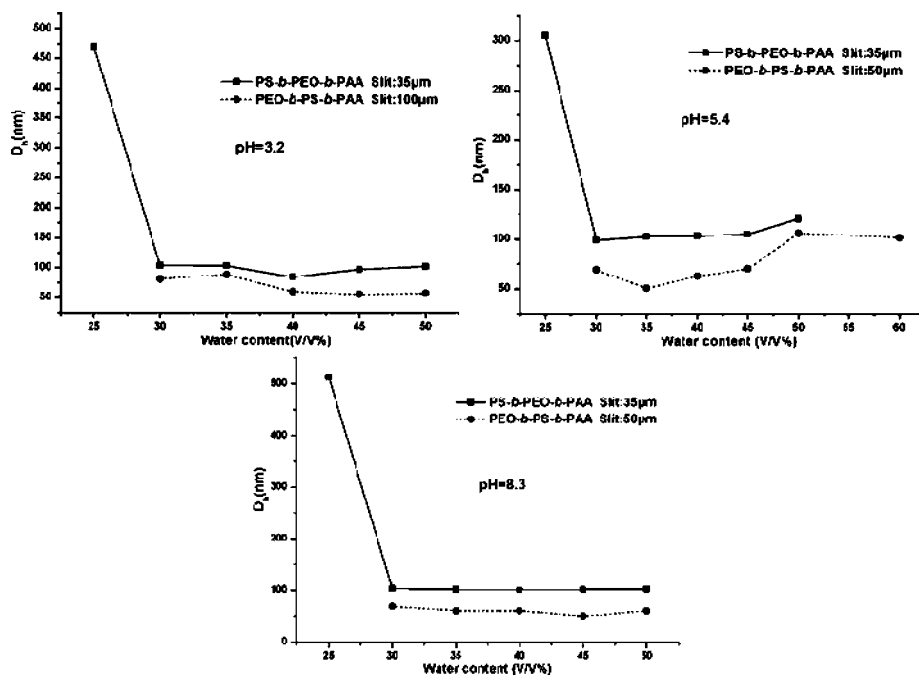
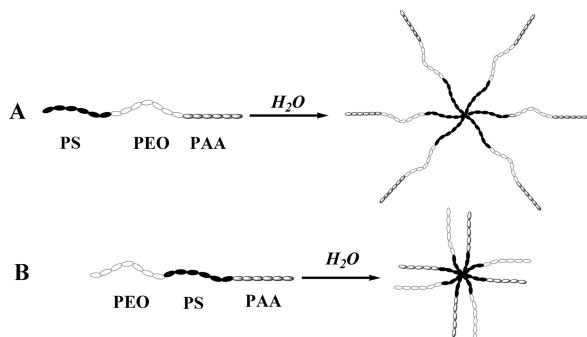


Figure 3. Aggregate size as a function of added water content at 1 mg/mL polymer concentration.

SCHEME 3: Schematic Representation of the Structures of the Spherical Micelles Formed by the Two Kinds of ABC Terpolymers in Dilute Solution



by amphiphilic diblock copolymers.^{40,41} But the phenomenon observed from PS-*b*-PEO-*b*-PAA system was quite different from previous references. To explain why the vesicles existed at relatively low water content (just above CWC), but disappeared at high water content, a schematic drawing (Scheme 4) about the kinetics of morphological transitions vs the water content was described.

Zhang and Eisenberg⁴² reported the relationship between the kinetics of morphological transitions and thermodynamic equilibration based on the adding rate of water. The main conclusion could be described as follows: (1) For the aggregates prepared by the water addition in their system, the kinetics are faster than the rate of water addition, and micellization will be under thermodynamic control when water content is below a certain water content (but above CWC). (2) When the water content increased, the aggregates can be easily frozen because the kinetics become slower than the rate of water addition. (3) When the water content is high enough, the kinetics have become extremely slow, and the thermodynamic state becomes unachievable, so that it is reasonable to postulate that the aggregates have been frozen completely.

In this article, the relationship between the kinetics and thermodynamics of morphology transition vs water addition was adopted to explain the formation of vesicles at 25% water

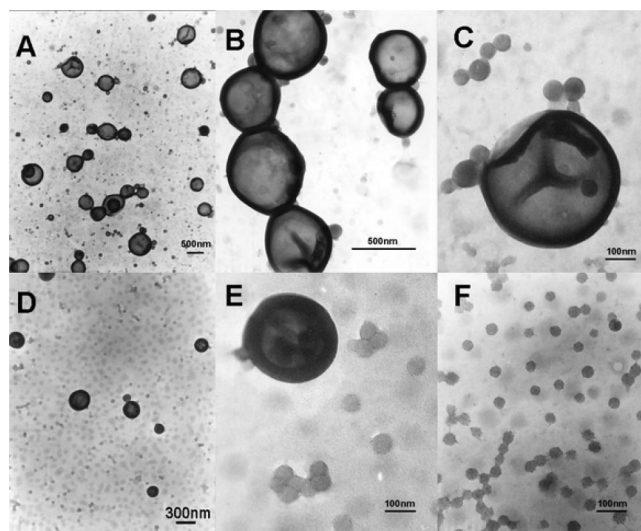


Figure 4. TEM pictures of the morphologies from the terpolymers PS-*b*-PEO-*b*-PAA at different water contents (pH value of the added water was 3.2): (A) 25%; (B, C) 25% with high magnification; (D) 30%; (E) 30% with high magnification; (F) 50%.

content for terpolymers PS-*b*-PEO-*b*-PAA. Figure 7 is an analogous schematic drawing of the kinetics of morphological transitions vs the water content for PS-*b*-PEO-*b*-PAA in H₂O/THF. The straight line A' represents the rate of water addition, curve B' represents schematically the relationship between the water content and the time needed for the system to reach thermodynamic equilibrium, and D₁', D₂', and E' represent three different phases. Because the coexistence of spherical micelles with tens of nanometers and vesicles with hundreds of nanometers was observed at 25% water content, which was just above its CWC (20%), it is postulated that the kinetics of aggregates transition was always slower than the rate of water addition. For the present system (PS-*b*-PEO-*b*-PAA), water contents 25% and 30% correspond to D₁' and D₂' in Figure 7. It means that the system needs a period of time to reach thermodynamic equilibration; the time may be a few hours or a couple of days. When the water content increased to 50%, the kinetics have

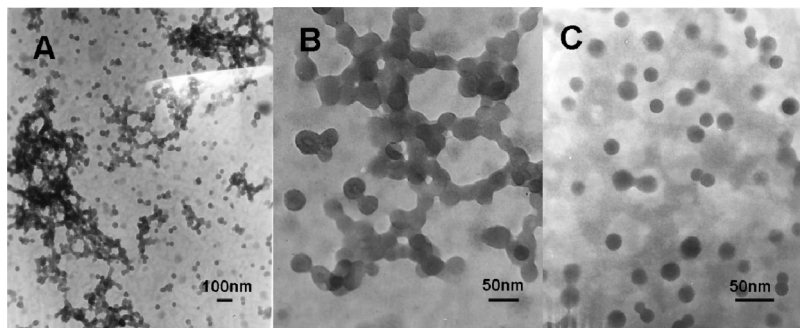


Figure 5. TEM pictures of the morphologies from the terpolymers PEO-*b*-PS-*b*-PAA at different water contents (pH value of the added water was 3.2): (A) 30%; (B) 30% with high magnification; (C) 50%.

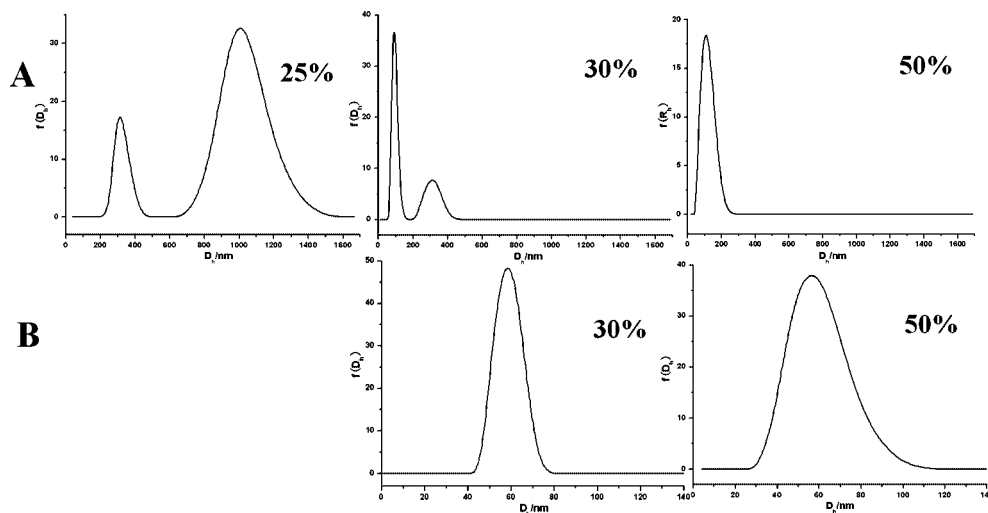
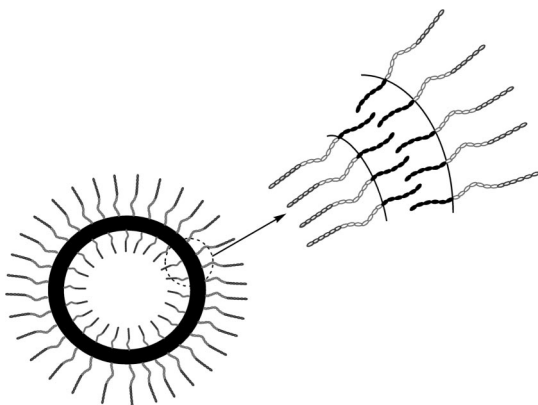


Figure 6. Hydrodynamic diameter distributions $f(D_h)$ of the aggregates at different water content (pH value of the added water was 3.2): (A) PS-*b*-PEO-*b*-PAA (slit: 35 μm); (B) PEO-*b*-PS-*b*-PAA (slit: 100 μm).

SCHEME 4: Schematic Representation of the Structures of Vesicles



become extremely slow, and the thermodynamic state becomes unachievable, which suggests that the aggregates have been frozen completely (Figure 7E'). That is why only spherical micelles can be observed in Figure 4F, and the size of spherical micelles is nearly the same it was obtained at the relatively lower water content (Figure 4A–C).

A tentative molecular packing model for the walls of the PS-*b*-PEO-*b*-PAA vesicles is shown in Scheme 4. In monolayer model, each PS-*b*-PEO-*b*-PAA molecule behaves as an amphiphilic diblock copolymer (AB type); therefore, the vesicle aggregates have an internal layer consisting of the PS core and outer shells of PEO-*b*-PAA as a result of the hydrophobic interaction. For PS₁₁₅-*b*-PEO₇₀-*b*-PAA₄₁, the contour length of

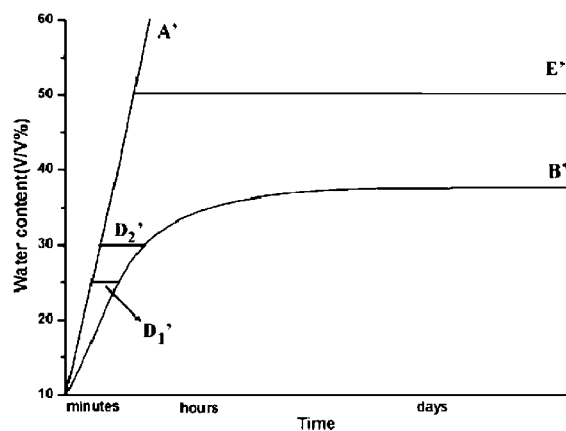


Figure 7. Relationship between morphological transitions vs the water content (PS-*b*-PEO-*b*-PAA in H₂O/THF).

PS block is estimated to be $\ll 28$ nm by $L = Nl$, where l is the length of repeat unit of PS block; its value is 0.25 nm, and N is the total number of units.⁴³ The total length of a bilayer structure of PS block approximately reaches to 56 nm, which is approachable to the thickness of the vesicle walls (50 nm) from TEM (Figure 4A–C). Thus, it could be concluded that the walls of vesicles showed a bilayer structure as indicated in Scheme 4. Similar structures were also observed by Zhou⁴⁴ and Battaglia.⁴⁵

The morphologies of PS-*b*-PEO-*b*-PAA and PEO-*b*-PS-*b*-PAA at different water contents with different pHs (5.4 and 8.3) are shown in the Supporting Information; the results are

consistent with what has been discussed at pH = 3.2. The block sequence of terpolymers may induce a different mechanism of morphology transition, and the concerned investigation is undergoing.

Conclusions

Based on the two terpolymers PS-*b*-PEO-*b*-PAA and PEO-*b*-PS-*b*-PAA with the same component, comparable molecular weight, but different block sequence, the influence of block sequence on the self-assembly of ABC terpolymers in selective solvent was investigated. It was found that a lower CWC and larger aggregate size were obtained for PS-*b*-PEO-*b*-PAA due to the different block sequence. When the water content reached 25%, vesicles and spherical micelles coexisted for PS-*b*-PEO-*b*-PAA, while the number and size of the vesicles decreased greatly as the water content increased, and vesicles disappeared as water content above 35%. But only spherical micelles were observed at all experimental conditions for PEO-*b*-PS-*b*-PAA. The relationship between the kinetics of morphological transitions and thermodynamic equilibration was used to explain this phenomenon. In our system, the kinetics of morphological transitions was always slower than the rate of water addition and became slower and slower with increase of water content. When water content was high enough, the thermodynamic state becomes unachievable. In conclusion, the aggregate behavior is influenced greatly by block sequence of ABC triblock copolymers.

Acknowledgment. We appreciate the financial support of the research from the National Science Foundation of China (Grant No. 20574010).

Supporting Information Available: Synthesis and characterization of triblock copolymer PS-*b*-PEO-*b*-PtBA and PEO-*b*-PS-*b*-PtBA. This material is available free of charge via the Internet at <http://pubs.acs.org>.

References and Notes

- (1) Babin, J.; Taton, D.; Brinkmann, M.; Lecommandoux, S. *Macromolecules* **2008**, *41*, 1384–1392.
- (2) Kuo, S. W.; Lee, H. F.; Huang, C. F.; Huang, C. J.; Chang, F. C. *J. Polym. Sci., Part A: Polym. Chem.* **2008**, *46*, 3108–3119.
- (3) Shvartzman-Cohen, R.; Florent, M.; Goldfarb, D.; Szleifer, I.; Yerushalmi-Rozen, R. *Langmuir* **2008**, *24*, 4625–4632.
- (4) Yu, B.; Li, B. H.; Jin, Q. H.; Ding, D.; Shi, A. C. *Macromolecules* **2007**, *40*, 9133–9142.
- (5) Zhang, L. F.; Yu, K.; Eisenberg, A. *Science* **1996**, *272*, 1777–1779.
- (6) Tsitsilianis, C.; Sfika, V. *Macromol. Rapid Commun.* **2001**, *22*, 647–651.
- (7) Voulgaris, D.; Tsitsilianis, C.; Esselink, F. J.; Hadziioannou, G. *Polymer* **1998**, *39*, 6429–6439.
- (8) Walther, A.; Goldmann, A. S.; Yelamanchili, R. S.; Drechsler, M.; Schmalz, H.; Eisenberg, A.; Muller, A. H. E. *Macromolecules* **2008**, *41*, 3254–3260.
- (9) Yu, K.; Zhang, L. F.; Eisenberg, A. *Langmuir* **1996**, *12*, 5980–5984.

- (10) Halperin, A. *Macromolecules* **1987**, *20*, 2943–2946.
- (11) Desbaumes, L.; Eisenberg, A. *Langmuir* **1999**, *15*, 36–38.
- (12) Yuan, J. J.; Li, Y. S.; Li, X. Q.; Cheng, S. Y.; Jiang, L.; Feng, L. X.; Fan, Z. Q. *Eur. Polym. J.* **2003**, *39*, 767–776.
- (13) Clarke, C. J.; Zhang, L. F.; Zhu, J. Y.; Yu, K.; Lennox, R. B.; Eisenberg, A. *Macromol. Symp.* **1997**, *118*, 647–655.
- (14) Park, S.; Wang, J. Y.; Kim, B.; Chen, W.; Russell, T. P. *Macromolecules* **2007**, *40*, 9059–9063.
- (15) Abbas, S.; Li, Z. B.; Hassan, H.; Lodge, T. P. *Macromolecules* **2007**, *40*, 4048–4052.
- (16) Gao, L. C.; Shi, L. Q.; An, Y. L.; Zhang, W. Q.; Shen, X. D.; Guo, S. Y.; He, B. L. *Langmuir* **2004**, *20*, 4787–4790.
- (17) Xu, C.; Wayland, B. B.; Fryd, M.; Winey, K. I.; Composto, R. J. *Macromolecules* **2006**, *39*, 6063–6070.
- (18) Bronstein, L. M.; Chernyshov, D. M.; Timofeeva, G. I.; Dubrovina, L. V.; Valetsky, P. M.; Obolonkova, E. S.; Khokhlov, A. R. *Langmuir* **2000**, *16*, 3626–3632.
- (19) Yu, K.; Eisenberg, A. *Macromolecules* **1998**, *31*, 3509–3518.
- (20) Bronstein, L. H.; Sidorov, S. N.; Valetsky, P. M.; Hartmann, J.; Colfen, H.; Antonietti, M. *Langmuir* **1999**, *15*, 6256–6262.
- (21) Chan, S. C.; Kuo, S. W.; Lu, C. H.; Lee, H. F.; Chang, F. C. *Polymer* **2007**, *48*, 5059–5068.
- (22) Bang, J.; Jain, S.; Li, Z. B.; Lodge, T. P. *Macromolecules* **2006**, *39*, 1199–1208.
- (23) Tsitsilianis, C.; Roiter, Y.; Katsampas, I.; Minko, S. *Macromolecules* **2008**, *41*, 925–934.
- (24) Zhu, Z. Y.; Xu, J.; Zhou, Y. M.; Jiang, X. Z.; Armes, S. P.; Liu, S. Y. *Macromolecules* **2007**, *40*, 6393–6400.
- (25) Wei, H.; Cheng, C.; Chang, C.; Chen, W. Q.; Cheng, S.; Zhang, X. Z.; Zhuo, R. X. *Langmuir* **2008**, *24*, 4564–4570.
- (26) Patrickios, C. S.; Hertler, W. R.; Abbott, N. L.; Hatton, T. A. *Macromolecules* **1994**, *27*, 930–937.
- (27) Fustin, C. A.; Abetz, V.; Gohy, J. F. *Eur. Phys. J. E* **2005**, *16*, 291–302.
- (28) Hadjichristidis, N.; Iatrou, H.; Pitsikalis, M.; Pispas, S.; Avgeropoulos, A. *Prog. Polym. Sci.* **2005**, *30*, 725–782.
- (29) Zhang, H.; Ni, P. H.; He, J. L.; Liu, C. C. *Langmuir* **2008**, *24*, 4647–4654.
- (30) Hu, J. W.; Liu, G. J.; Nijkang, G. *J. Am. Chem. Soc.* **2008**, *130*, 3236–3237.
- (31) Liu, F.; Eisenberg, A. *J. Am. Chem. Soc.* **2003**, *125*, 15059–15064.
- (32) Yu, G. E.; Eisenberg, A. *Macromolecules* **1998**, *31*, 5546–5549.
- (33) Chen, W. Y.; Alexandridis, P.; Su, C. K.; Patrickios, C. S.; Hertler, W. R.; Hatton, T. A. *Macromolecules* **1995**, *28*, 8604–8611.
- (34) Trifitaridou, A. I.; Vamvakaki, M.; Patrickios, C. S. *Polymer* **2002**, *43*, 2921–2926.
- (35) Kyriacou, M. S.; Hadjiyannakou, S. C.; Vamvakaki, M.; Patrickios, C. S. *Macromolecules* **2004**, *37*, 7181–7187.
- (36) Patrickios, C. S.; Lowe, A. B.; Armes, S. P.; Billingham, N. C. *J. Polym. Sci., Part A: Polym. Chem.* **1998**, *36*, 617–631.
- (37) Zhang, Y.; Pan, M. G.; Liu, C.; Huang, J. L. *J. Polym. Sci., Part A: Polym. Chem.* **2008**, *46*, 2624–2631.
- (38) Lin, W. C.; Fu, Q.; Zhang, Y.; Huang, J. L. *Macromolecules* **2008**, *41*, 4127–4135.
- (39) Zhang, L. F.; Eisenberg, A. *Polym. Adv. Technol.* **1998**, *9*, 677–699.
- (40) Zhang, L. F.; Eisenberg, A. *J. Am. Chem. Soc.* **1996**, *118*, 3168–3181.
- (41) Shen, H. W.; Eisenberg, A. *J. Phys. Chem. B* **1999**, *103*, 9473–9487.
- (42) Zhang, L. F.; Eisenberg, A. *Macromolecules* **1999**, *32*, 2239–2249.
- (43) Teraoka, I. *Polymer Solutions*; John Wiley & Sons: New York, 2002.
- (44) Zhou, Y. F.; Yan, D. Y. *Angew. Chem., Int. Ed.* **2004**, *43*, 4896–4899.
- (45) Battaglia, G.; Ryan, A. J. *J. Am. Chem. Soc.* **2005**, *127*, 8757–8764.

JP8053444